Linearly extended hybrid tetrathiafulvalene analogues with bridged dithienylethylene π-conjugating spacers

Hugues Brisset,[a] Soazig Le Moustarder,[a] Philippe Blanchard,[a] Bertrand Illien,[a] Amédée Riou,[a] Jesus Orduna,[b] Javier Garin[b] and Jean Roncali*[a]

[a]*Ingénierie Moléculaire et Matériaux Organiques, CNRS UMR 6501, Université d'Angers, 2 Bd Lavoisier, 49045 Angers, France*
[b]*Laboratorio de Quimica Organica Universidad de Zaragoza, Zaragoza, Spain*

New linearly extended π-electron donors based on bridged dithienylethylene (DTE) end-capped with diversely substituted 1,3-dithiol-2-ylidene electron-releasing groups have been synthesized by Wittig–Horner olefination of appropriate aldehydes. Cyclic voltammetry shows that whereas the unbridged analogues are directly oxidized to the dication state through a two-electron transfer, rigidification of the DTE spacer leads to the splitting of the two-electron wave into two successive one-electron steps due to the decrease of the potential corresponding to the formation of the cation radical. This unusual electrochemical behaviour is interpreted with the help of theoretical calculations which suggest that these effects are related to the enhanced electron delocalization resulting from the rigidification of the DTE spacer. This conclusion is supported by an X-ray diffraction structural analysis which reveals that in addition to a fully planar conformation stabilized by intramolecular S···S interactions, the bridging of the DTE spacer leads to a significant reduction of bond length alternation.

Linear π-conjugated systems end-capped with 1,3-dithiol-2-ylidene groups have recently emerged as a growing class of organic compounds with specific electronic properties.[1] Interest in these systems was initially motivated by the increased dimensionality and hence improved electrical properties anticipated for the corresponding cation-radical salts, in the general frame of the chemistry of extended tetrathiafulvalene (TTF) analogues.[2] However, more recent work has shown that these hybrid π-conjugated systems are also potentially interesting as small-bandgap molecular semiconductors[3] or as building blocks for push–pull or push–push molecules for quadratic or cubic non-linear optics.[4,5] Since these various applications are closely related to the delocalization of π-electrons, the design of a π-conjugating spacer group showing optimal electron transmission properties associated with good thermal and photochemical stability appears to be a priority.

In this context oligoheteroarylenevinylene spacers have recently emerged as a good trade-off between the efficient but unstable polyalkenic systems[6] and the more stable poly(hetero)aromatic ones which present excessive π-electron confinement.[7]

We have already reported the synthesis of linearly extended TTF analogues (LETTFs) based on oligoheteroarylenevinylenes end-capped with 1,3-dithiol-2-ylidene units.[8] Whereas for LETTFs involving oligothiophenes, internal rotational disorder leads to rapid saturation of the effective conjugation beyond a bithiophenic spacer, *i.e.* eight conjugated carbons,[1e] such a saturation has not been observed yet even for the longest known LETTFs built around a tetrathienylenevinylene spacer (22 conjugated carbons).[9]

Recently, we have shown that the bridging of the thiophene rings with the central ethylene linkage of dithienyethylene (DTE) produces a 0.40 eV decrease of the bandgap of the resulting electrogenerated polymer.[10] As a further step we report here the synthesis of new LETTFs built by grafting the 1,3-dithiol-2-ylidene moiety to both ends of a bridged DTE spacer **1a–c**. Comparison of the electrochemical properties of these new π-donors with those of their non bridged analogues **4a–c** shows that rigidification of the spacer leads to an increase of π-donor ability with a stabilisation of the cation radical state. These results are discussed in the light of theoretical and X-ray structural analyses which indicate that the bridging of the DTE spacer produces a decrease in bond length alternation resulting in an enhanced π-electron delocalization.

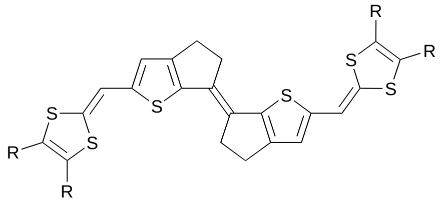

1a–c

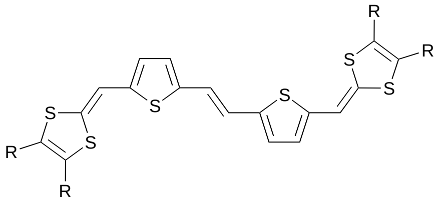

4a–c

a R = CO_2Me
b R = SMe
c R = Pr^n

Results and Discussion

The synthesis of compounds **1a–c** is depicted in Scheme 1. Bridged dithienyethylene **3** has been prepared by McMurry coupling of 4,5-dihydro-6*H*-cyclopenta[*b*]thiophen-6-one[11] as already described.[10,12] Dilithiation of **3** using *n*-butyllithium followed by reaction with DMF afforded the dicarbaldehyde **2** in 81% yield. The target compounds **1a–c** were then obtained in 45–50% yield by double Wittig–Horner olefination of **2** using an appropriately substituted phosphonium salt **5a** or phosphonate anions derived from the dithiolium salts **6b,c**.[13]

The cyclic voltammograms (CV) of **1a** and **1c** in methylene chloride are shown in Fig. 1. The CV of **1a** exhibits two reversible one-electron oxidation waves with anodic peak

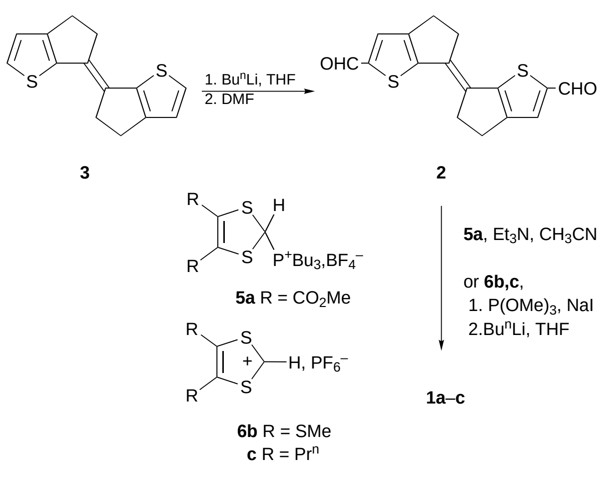

Scheme 1

potentials E_{pa1} and E_{pa2} at 0.49 and 0.65 V corresponding to the successive generation of the cation radical and dication.

As expected, replacement of the electron-withdrawing CO_2Me by the electron-releasing SMe and especially *n*-propyl groups leads to a negative shift of E_{pa1} and E_{pa2} while the potential difference $E_{pa2}-E_{pa1}$ decreases from 0.16 to 0.09 V, indicating a reduction of the on-site coulombic repulsion between positive charges in the dication [Fig. 1(*b*) and Table 1]. The comparison of the CV data of compounds **1** with those of their analogues built around a single thiophene ring[1b] reveals a *ca.* 0.20 V negative shift of the peak potentials thus confirming that the insertion of the bridged DTE spacer leads to a significant improvement of the π-donor ability.

However, comparison of the CV data of compounds **1a–c** with those of **4a–c** containing a classical DTE spacer shows that the bridging of the spacer produces two noticeable changes. Firstly, E_{pa1} undergoes a 70–100 mV negative shift which is indicative of enhanced π-donor ability. However, whereas compounds **4b** and **4c** are directly oxidized into their dication state through a single step two-electron transfer,[9] rigidification of the DTE spacer leads to the splitting of this two-electron wave into two successive one-electron oxidation steps. A closer examination of the data in Table 1 shows that for each compound **1**, decoalescence and hence the increase of $E_{pa2}-E_{pa1}$ results from the negative shift of E_{pa1} while E_{pa2} values remain similar to those of the unbridged analogues. This result implies that the bridging of the spacer leads to a stabilization of the cation radical state.

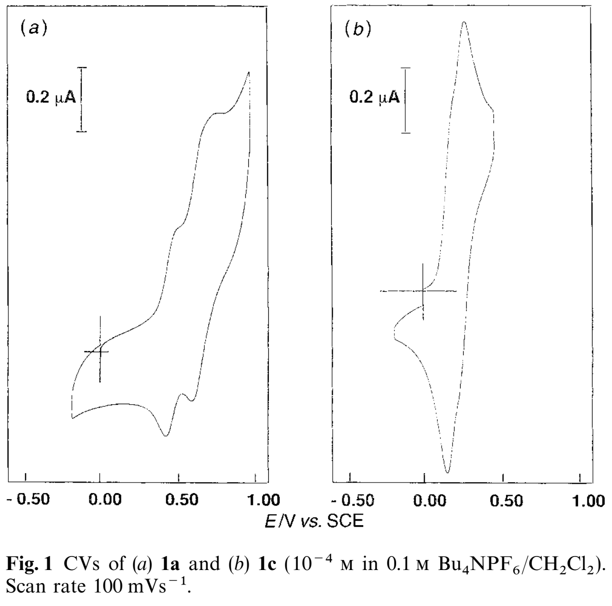

Fig. 1 CVs of (*a*) **1a** and (*b*) **1c** (10^{-4} M in 0.1 M Bu_4NPF_6/CH_2Cl_2). Scan rate 100 mV s^{-1}.

Table 1 Electrochemical data for compounds **1** and **4**,[b] 10^{-4} M in 0.1 M Bu_4NPF_6/CH_2Cl_2. Scan rate 100 mV s^{-1}, all potentials in V *vs.* SCE

compound	E_{pa1}/V	E_{pa2}/V	$E_{pa2}-E_{pa1}$/V
1a	0.49	0.65	0.16
1b	0.33	0.45	0.11
1c	0.22	0.31	0.09
4a[b]	0.59[a]	0.66	0.07
4b[b]	0.43	—	0.00
4c[b]	0.29	—	0.00

[a]Shoulder. [b]From ref. 8(*a*).

Previous work on LETTFs containing polyalkenic or oligoheteroarylenelvinylenes π-conjugating spacers has shown that the lengthening of the spacer group produces a negative shift of E_{pa1} and E_{pa2} together with a decrease of their difference.[1a,1e,8] Thus, beyond a certain conjugation length which depends on the structure of the spacer, direct formation of the dication state through a two-electron transfer occurs.[1a,8,9] In this context, the behaviour of compounds **1** appears as rather surprising since, as far as we know, it is the first time that a decrease in oxidation potential is associated with an increase of $E_{pa2}-E_{pa1}$ and hence a stabilization of the cation radical instead of the dication.

Previous work has shown that the bridging of DTE leads to a negative shift of E_{pa1} and E_{pa2} from 1.10 and 1.40 to 0.72 and 1.16 V, respectively while $E_{pa2}-E_{pa1}$ increases from 0.30 to 0.44 V.[10] This increase in the HOMO level leads to a 0.40 eV reduction of the HOMO–LUMO gap (Δ*E*) of the molecule and of the bandgap of the resulting polymer. The great similarity between these effects and those observed for **1a–c** clearly shows that the bridging of the DTE spacer is the origin of their unusual electrochemical properties. The smaller magnitude of the effects observed here can be related to the fact that the 1,3-dithiole moieties provide the major contribution to the HOMO level in LETTFs.[1a,8]

In a recent joint X-ray diffraction and theoretical analysis of bridged DTEs, we have shown that the reduction of Δ*E* induced by the bridging of DTE results from a decrease of bond length alternation.[12] As widely acknowledged, this parameter represents the main cause for the existence of a finite bandgap in linearly π-conjugated systems.[14] In order to analyse the role of bond length alternation in the electronic properties of compounds **1**, the structure of a single crystal of **1c** has been investigated by X-ray diffraction. The ORTEP view in Fig. 2 shows that the molecule is non-centrosymmetric and adopts a fully planar geometry except for the *n*-propyl chains that lie outside the plane of the molecule. While the planarity of the conjugated DTE spacer is ensured by the bridge, both lateral parts of the molecule are rigidified by strong 1,5 intramolecular S···S interactions between the sulfur atom of the thiophene ring and a sulfur of the 1,3-dithiole moiety. The S1···S3 and S4···S5 distances (3.154 and 3.171 Å respectively) are larger than a covalent S—S bond (2.04 Å) but shorter than twice the van der Waals radius of sulfur (3.60 Å). Such interactions have already been observed for related compounds.[1e,8,15]

The crystal structure of **1c** involves columns of molecules along the [001] crystallographic direction (Fig. 3). The molecules centrosymmetrically related are stacked in a head-to-tail way along the *c* axis. Molecules within a column are equidistant with an average separation of 3.95 Å. The contact distances between molecules in neighbouring columns are too large to take any interaction into account.

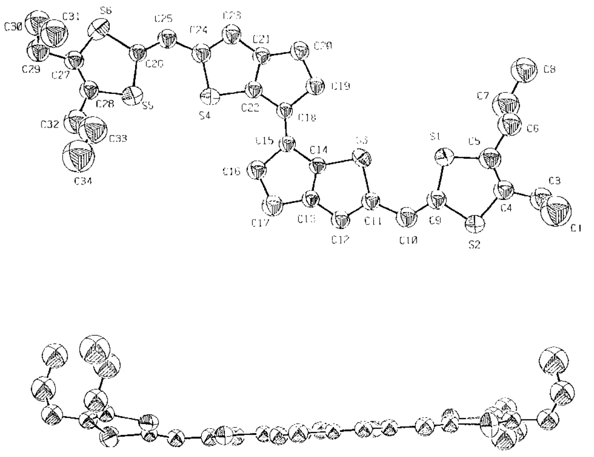

Fig. 2 ORTEP view of **1c**

Table 2 Bond distances in the DTE conjugated path (see formulae for bond labelling)

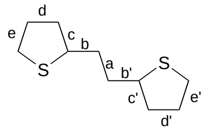

bond	DTE[a]	**7**[b]	**1c**
e	1.351(8)	1.350(1)	1.36(2)
d	1.44(1)	1.409(8)	1.41(2)
c	1.40(1)	1.356(8)	1.37(2)
b	1.457(7)	1.440(7)	1.44(2)
a	1.309(8)	1.335(6)	1.33(2)
b′	1.447(7)	1.440(7)	1.43(1)
c′	1.40(1)	1.356(8)	1.34(2)
d′	1.44(1)	1.409(8)	1.40(2)
e′	1.351(8)	1.350(1)	1.38(1)
δr/Å	0.096	0.078	0.064

[a] From ref. 16. [b] From ref. 12.

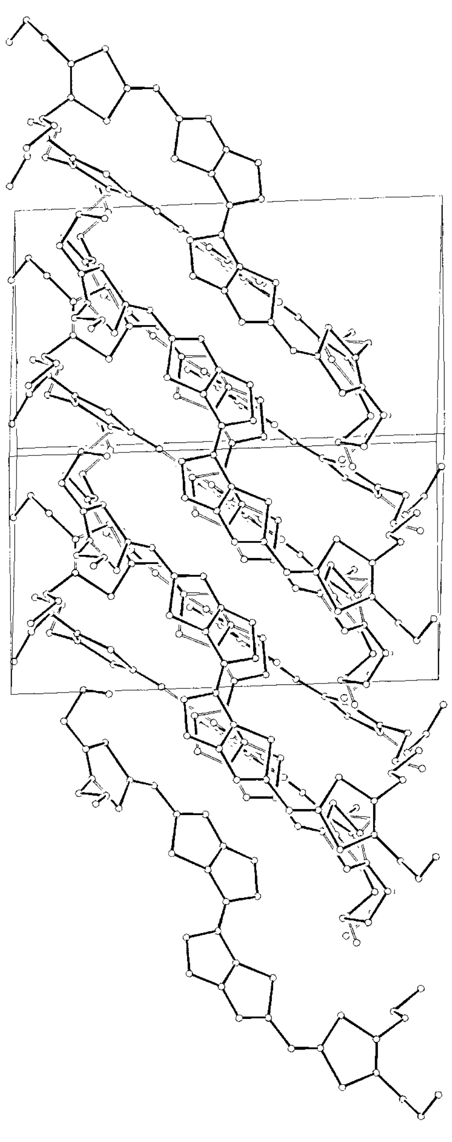

Fig. 3 Crystal structure of **1c**

Comparison of the bond distances in the DTE moiety for DTE,[16] 4,4′-dibutyl-6,6′-bi(4,5-dihydro-6*H*-cyclopenta[*b*]thienylidene) **7**, a substituted analogue of **3**,[12] and **1c** shows that the presence of the bridge produces a lengthening of the a, e and e′ double bonds and a compression of the b, d, b′ and d′ single bonds (Table 2).

An important consequence of these bond length modifications is a significant decrease of bond length alternation expressed as the difference between the average length of single and double bonds (δr). Thus, as shown in Table 2, δr decreases from 0.096 Å for DTE to 0.075 Å for **7**[12] and 0.064 Å for **1c**. The smaller δr value obtained for **1c** might be related to the further constraint imposed on the DTE moiety by the 1,5 intramolecular S···S interactions. Although the large uncertainties related to the rather limited quality of the **1c** crystal mean that these data should be considered with care, the trend expressed here confirms that the reduction of bond length alternation already observed for **7** persists when this system is used as π-conjugating spacers in LETTFs.

These results allow us to propose a possible explanation for the peculiar electrochemical behaviour of compounds **1.** Oxidation of **1** and **4** to the cation radical state induces geometrical changes in the conjugated path, the thiophene rings adopt a quinoid structure while the central ethylene linkage acquires the character of an essentially single bond (Scheme 2).

In this context, the changes in bond distances induced by the bridging of the DTE moiety and in particular the compression of bonds b, d, b′, d′ and the lengthening of bonds a and e contribute to prefigure the final geometry of the cation radical. Consequently, formation of the cation radical becomes easier and thus requires less energy, in agreement with the observed decrease of E_{pa1}. On the other hand, since there is much less difference between the geometries of $\mathbf{1}^{\cdot +}$ and $\mathbf{4}^{\cdot +}$ than between their respective neutral forms, the bridging of the DTE spacer has much less influence on the energy required by the second oxidation step, which is consistent with for the quasi invariance of E_{pa2}.

In order to gain more information on this question, theoretical calculations have been performed for the neutral, cation radical and dication forms of compounds **1b** and **4b.** The geometry of neutral and dicationic species have been optimized using the PM3/RHF method and that of the cation radical with the PM3/UHF method. Table 3 lists the computed values of the ionization potential (E_i), dipole moment (μ), heat of

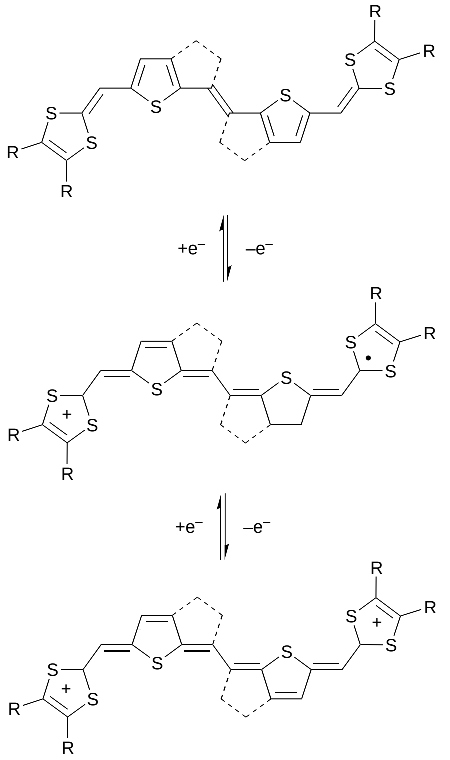

Scheme 2

Table 3 Computed values of ionization potential (E_i), dipole moment (μ), heat of formation (ΔH_f) and degree of bond length alternation (δr) for compounds **4b** and **1b** and their cationic species

compound	E_i/eV	μ/D	ΔH_f/kcal mol^{-1}	δr/Å
1b	7.82	0.1	177.9	0.062
1b$\cdot^+$		0.2	331.7	−0.030
1b^{++}		0.0		−0.098
4b	7.94	0.1	180.7	0.063
4b$\cdot^+$		24	339.4	−0.018
4b^{++}		0.2		−0.113

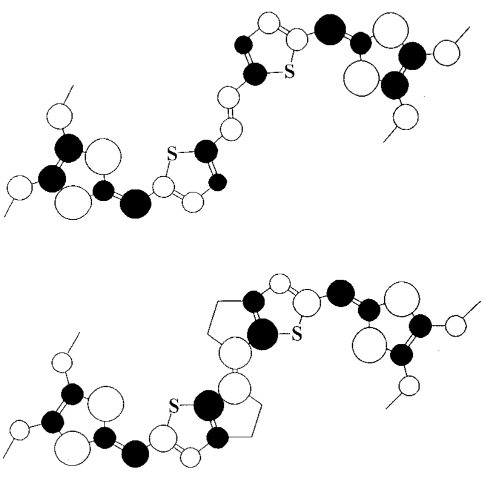

Fig. 4 AO coefficients in HOMO of (*a*) **4b** and (*b*) **1b**

formation (ΔH_f). The δr values used refer only to the DTE system.

The E_i value for **1b** is found 0.12 eV lower than for **4b**; this difference exactly matches that found betwen E_{pa1} values (Table1), but this agreement might be fortuitous. The geometries of **1b** and **4b** are very symmetrical and present a quasi inversion centre leading to a dipole moment close to zero. The computed geometries do not provide evidence for the effect of the bridge and show only a slight difference in δr (0.062 and 0.063 Å for **1b** and **4b** respectively). The fact that the noticeable difference in δr indicated by X-ray data is not found here may reflect a limitation of the computing method used. The *ca.* 12 kJ mol^{-1} decrease of ΔH_f observed for **1b** suggests that, as expected, the presence of the bridge enhances the stability of the molecule. As shown in Fig. 4, whereas for **4b** the highest coefficients of the HOMO are located on the 1,3-dithiole units, for **1b** the distribution is more homogeneous which suggests a better delocalization of π-electrons over the whole molecule. The data of the cation radical show that in both cases δr becomes negative, in agreement with the expected inversion of bond alternation (see Scheme 2). Oxidation of **4b** into **4b**$\cdot^+$ leads to a large increase in the dipole moment, consistent with a strong localization of the positive charge in one 1,3-dithiole unit. In contrast, there is practically no change in the μ value between **1b** and **1b**$\cdot^+$ which suggests that the positive charge is delocalized over the entire molecule. This result which agrees well with the reduced δr value of **1b** appears consistent with the observed stabilization of the cation radical as indicated by CV data.

Conclusion

To summarize, new conjugated π-donors incorporating bridged DTE spacers have been synthesized. The combined effects of the bridge in the spacer and of 1,5-intramolecular S···S interactions lead to a fully planar rigid structure with reduced bond length alternation. The geometrical modifications induced by the rigidification of the DTE spacer result in the splitting of the two-electron oxidation wave observed for the unbridged systems into two successive one-electron steps with a concomitant decrease of the first oxidation potential. This rather unusual behaviour is attributed to a stabilization of the cation radical state associated with an enhanced delocalization of the positive charge.

Experimental

Electrochemical experiments were carried out with a PAR 273 Potentiostat-Galvanostat in a three-electrode single-compartment cell equipped with platinum microelectrodes of 7.85×10^{-3} cm^2 area, a platinum wire counter electrode and a saturated calomel reference electrode (SCE). Solutions were deaerated by nitrogen bubbling prior to each experiment which was run under a nitrogen atmosphere.

X-Ray structural analyses

Crystal data for 1c. $C_{34}H_{40}S_6$ M_W 641.08, monoclinic, $P2_1/c$, $Z=4$, $a=16.618(7)$, $b=17.850(11)$, $c=11.005(9)$ Å, $\beta=92.25(5)°$, $V=3262(6)$ Å^3, $\lambda=0.71069$ Å.

Data collection. Data collection by the zig-zag ω scan technique, $2°\leqslant\Theta\leqslant25°$, $t_{max}=40$ s, range h, k, l (h 0,13; k 0,21; l −19,19), intensity controls without appreciable decay (0.2%) gives 6202 reflections from which 1279 were independent with $I>3\sigma(I)$.

Structure refinement. After Lorentz and polarisation corrections the structure was solved with direct methods (SIR) which reveal all the non-hydrogen atoms. After isotropic and anisotropic refinement of all the C and S atoms respectively, the coordinates of H atoms were determined using the HYDRO program. The whole structure was refined by the full-matrix least-squares techniques {use of *F* magnitude; U_{ij} for S atoms, *x*, *y*, *z* and *B* fixed for H; 191 variables and 1276 observations, weighting $w=1/\sigma(F_0)^2=4(F_0)^2/[\sigma(I)^2+(0.04\ F_0{}^2)^2]$} with the resulting $R=0.061$, $R_w=0.060$.

Theoretical calculations

The semi-empirical PM3 method[17] has been parametrized to reproduce gas-phase properties, *i.e.* geometry, dipole moment, ionization potential and heat of formation. The PM3 method was used in the framework of the HYPERCHEM 5.0 package.[18] The geometry of **1b**, **4b** and of their dication has been optimized at the RHF level of theory and the geometry of **1b**$\cdot^+$ and **4b**$\cdot^+$ has been computed at the UHF level. All optimized geometries are almost planar and have root-mean-square gradient values lower than 0.1 kcal mol^{-1}Å^{-1} (1 cal = 4.184 J). Ionization potential values were obtained through Koopmans' theorem.[19]

6,6′-Bi(4,5-dihydro-6*H*-cyclopenta[*b*]thienylidene) 3. Compound **3** was synthesized according to a previously described procedure.[10,12]

2,2′-Diformyl-6,6′-Bi(4,5-dihydro-6*H*-cyclopenta[*b*]thienylidene 2. In a round-bottomed flask equipped with a dropping funnel and nitrogen inlet was added **3** (0.1 g, 0.41 mmol) in 20 ml of dry tetrahydrofuran (THF). The mixture was cooled to 0 °C and BuLi (1.6 M in hexanes) (0.54 ml, 0.86 mmol) was added dropwise. After 15 min stirring at 0 °C, anhydrous dimethylformamide (DMF) (0.20 ml, 2.34 mmol) was added; the mixture was allowed to warm to room temp. and stirred for 30 min. Water was then added and the mixture extracted with diethyl ether. The organic phase was dried over $CaCl_2$. Removal of the solvent and column chromatography of the residue (silica gel, CH_2Cl_2) gave 0.10 g (81%) of a red powder, mp 198–200 °C, δ_H ($CDCl_3$) 3.00–3.15 (m, 8H), 7.79 (s, 2H), 9.86 (s, 2H). ν/cm^{-1} (KBr) 1650 (C=O). MS *m*/*z* 300 ($M^{\cdot+}$ 100).

2,2′-Bis[4,5-bis(methoxycarbonyl)-1,3-dithiol-2-ylidenemethyl]-6,6′-bi(4,5-dihydro-6*H*-cyclopenta[*b*]thienylidene) 1a. To a stirred solution of phosphonium salt **5a** (1 g, 2 mmol) and dialdehyde **2** (0.1 g, 0.33 mmol) in 20 ml of CH_3CN, triethylamine (0.32 ml, 2.33 mmol) was added dropwise. After 2 h stirring at room temp., the solvent was removed by evaporation and the residue purified by column chromatography (silica gel, light petroleum–ethyl acetate 9 : 1) to give 67 mg (30%) of a dark green powder with a metallic lustre, mp > 280 °C, δ_H ($CDCl_3$) 2.83–3.45, (m, 8H), 3.87, (s, 6H), 3.89 (s, 6H), 6.59 (s, 2H), 6.72 (s, 2H). MS (EI) *m*/*z* 704 ($M^{\cdot+}$ 100). ν/cm^{-1} (KBr) 1705 and 1737 (C=O). UV–VIS (CH_2Cl_2) λ_{max} nm (log ε) 469 (3.99), 501 (3.97).

2,2′-Bis[4,5-bis(methylthio)-1,3-dithiol-2-ylidenemethyl]-6,6′-bi(4,5-dihydro-6*H*-cyclopenta[*b*]thienylidene) 1b. In a round-bottomed flask equipped with a dropping funnel and nitrogen inlet were introduced dithiolium salt **6b** (0.28 g, 1 mmol), trimethyl phosphite (0.12 ml, 1 mmol) and KI (0.15 g, 1 mmol) in 3 ml of acetonitrile. After 2 h stirring at room temp., evaporation of the solvent and excess of trimethyl phosphite left the phosphonate as an oil. Dry THF (3 ml) and dicarbaldehyde **2** (0.08 g, 0.25 mmol) were then added and the mixture cooled to 0 °C. *n*-Butyllithium (0.63 ml, 2 mmol) (1.6 M in hexanes) was added dropwise, and the mixture stirred for 2 h at room temp. Upon addition of methanol a red precipitate was formed which is filtered, washed with methanol–diethyl ether and dried. Yield 0.07 g (45%), mp 261–263 °C. δ_H ($CDCl_3$) 2.46 (s, 6H), 2.48 (s, 6H), 2.90–3.10 (m, 4H), 3.20–3.35 (m, 4H), 6.62 (s, 2H), 6.68 (s, 2H). MS *m*/*z* 657 ($M^{\cdot+}$), HRMS calc. for $C_{26}H_{24}S_{10}$ 655.9085, found 655.9064. UV–VIS (CH_2Cl_2) λ_{max}/nm (log ε) 481(4.84), 516 (4.82)

2,2′-Bis(4,5-dipropyl-1,3-dithiol-2-ylidenemethyl)-6,6′-bi(4,5-dihydro-6*H*-cyclopenta[*b*]thienylidene) 1c. This compound was prepared using the same procedure from dithiolium salt **6c** (0.90 g (2.72 mmol), trimethyl phosphite (0.32 ml, 2.72 mmol), KI, (0.41 g, 2.72 mmol) and dicarbaldehyde **2** (0.20 g, 0.67 mmol). After the usual work-up the product was purified by column chromatography (silica gel, CH_2Cl_2). Yield (47%), red powder, mp 175–180 °C. δ_H ($CDCl_3$) 1.39–1.82 (m, 24H), 2.21–2.71 (m, 8H), 6.88 (s, 2H), 7.29 (s, 2H). δ_C ($CDCl_3$) 13.51, 13.63, 22.65, 29.66, 30.54, 35.27, 106.18, 118.47, 122.96, 127.55, 128.78, 128,92, 131.86. MS *m*/*z* 641 ($M\cdot^+$100), 455 (17%), 320 (21%), 111(34%). HRMS calc. for $C_{34}H_{40}S_6$ 640.1454, found 640.1442. UV–VIS (CH_2Cl_2) λ_{max}/nm (log ε) 484(4.83), 520(4.83).

References

1 (*a*) T. Sugimoto, H. Awaji, I. Sugimoto, Y. Misaki, T. Kawase, S. Yoneda and Z. Yoshida, *Chem. Mater.*, 1989, **1**, 535; (*b*) A. Benahmed-Gasmi, P. Frère, B. Garrigues, A. Gorgues, M. Jubault, R. Carlier and F. Texier, *Tetrahedron Lett.*, 1992, **33,** 6457; (*c*) T. K. Hansen, M. V. Lakshmikantam, M. P. Cava, R. E. Niziurski-Mann, F. Jensen and J. Becher, *J. Am. Chem. Soc.*, 1992, **114**, 5035; (*d*) J. Roncali, M. Giffard, P. Frère, M. Jubault and A. Gorgues, *J. Chem. Soc., Chem. Commun.* 1993, 689; (*e*) J. Roncali, L. Rasmussen, C. Thobie-Gautier, P. Frère, H. Brisset, M. Sallé, J. Becher, O. Simonsen, T. K. Hansen, A. Benahmed-Gasmi, J. Orduna, J. Garin, M. Jubault and A. Gorgues, *Adv. Mater.*, 1994, **6,** 841.

2 (*a*) M. R. Bryce, *J. Mater. Chem.*, 1995, **5,** 1481; (*b*) M. Adam and K. Müllen, *Adv. Mater.*, 1994, **6**, 439; (*c*) Y. Misaki, N. Higuchi, H. Fujiwara, T. Yamabe, T. Mori, H. Mori and S. Tanaka, *Angew. Chem., Int. Ed. Engl.*, 1995, **34,** 1222.

3 H. Brisset, C. Thobie-Gautier, M. Jubault, A. Gorgues and J. Roncali, *J. Chem. Soc., Chem. Commun.*, 1994, 1765.

4 (*a*) V. P. Rao, K.-Y. Jen, K. Y. Wong and K. J. Drost *Tetrahedron Lett.*, 1993, **34**, 1747; (*b*) U. Schöbert, J. Salbeck and J. Daub, *Adv. Mater.*, 1992, **4**, 41; (*c*) K.-Y. Jen, V. P. Rao, K. Y. Wong and K. J. Drost, *J. Chem. Soc., Chem. Commun.*, 1993, 90.

5 (*a*) M. Sylla, J. Zaremba, R. Chevalier, G. Rivoire, A. Khanous and A. Gorgues, *Synth. Met.*, 1993, **59**, 111; (*b*) T. T. Nguyen, M. Sallé, B. Sahraoui, M. Sylla, J. P. Bourdin, G. Rivoire and J. Zaremba, *J. Modern Opt.*, 1995, **42**, 2095.

6 (*a*) I. Cabrera, O. Althoff, H.-T. Man and H. N. Yoon, *Adv. Mater.*, 1994, **6**, 43; (*b*) M. Blanchard-Desce, C. Runser, A. Fort, M. Barzoukas, J. M. Lehn, V. Bloy and V. Alain, *Chem. Phys.*, 1995, **199**, 253; (*c*) H. Gibson and J. Pochan, *Macromolecules*, 1991, **24**, 4834.

7 (*a*) S. Gilmour, R. A. Montgomery, S. R. Marder, L.-T. Cheng, K.-Y. Jen, Y. Cai, J. W. Perry and L. R. Dalton, *Chem. Mater.*, 1994, **6**, 1603; (*b*) V. Hernandez, C. Castiglioni, M. Del Zopo and G. Zerbi, *Phys. Rev. B*, 1994, **50**, 9815.

8 (*a*) E. Elandaloussi, P. Frère, J. Roncali, P. Richomme, M. Jubault and A. Gorgues, *Adv. Mater.*, 1995, **7**, 390; (*b*) A. Benahmed-Gasmi, P. Frère, E. Elandaloussi, J. Roncali, J. Orduna, J. Garin, M. Jubault, A. Riou and A. Gorgues, *Chem. Mater.*, 1996, **8**, 2291; (*d*) E. Elandaloussi, P. Frère, A. Benahmed-Gasmi, A. Riou, A. Gorgues and J. Roncali, *J. Mater. Chem.*, 1996, **6**, 1859.

9 E. Elandaloussi, P. Frère and J. Roncali, *Tetrahedron Lett.* 1996, **37**, 6121.

10 J. Roncali, Thobie-Gautier, E. Elandaloussi and P. Frère, *J. Chem. Soc., Chem. Commun.*, 1994, 2249.

11 D. W. H. MacDowell, T. B. Patrick, B. K. Frame and D. L. Ellison, *J. Org. Chem.*, 1967, **32,** 1227.

12 (*a*) H. Brisset, P. Blanchard, B. Illien, A. Riou and J. Roncali, *Chem. Commun.*, 1997, 569 (*b*) P. Blanchard, H. Brisset, B. Illien, A. Riou and J. Roncali, *J. Org. Chem.*, 1997, **62**, 2401.

13 (*a*) K. Akiba, K. Ishikawa and N. Inasoto, *Bull. Chem. Soc. Jpn.*, 1978, **51**, 2674; (*b*) T. K. Hansen, M. V. Lakshmikantham, M. P. Cava, R. M. Metzger and J. Becher, *J. Org. Chem.*, 1991, **56,**

2720; (*c*) A. J. Moore, M. R. Bryce, D. T. Ando and M. B. Hursthouse, *J. Chem. Soc., Chem. Commun.*, 1991, 320.

14 J. Roncali, *Chem. Rev.*, 1997, **97**, 173.

15 T. K. Hansen, M. R. Bryce J. A. K. Howard and D. S. Yffit, *J. Org. Chem.*, 1994, **59**, 5324.

16 G. Ruban and D. Zobel, *Acta Crystallogr., Sect. B*, 1975, **31,** 2632.

17 (*a*) J. J. P. Stewart, *J. Comput. Chem.*, 1989, **10**, 209; (*b*) J. J. P. Stewart, *J. Comput. Chem.*, 1989, **10**, 221.

18 HYPERCHEM 5.0, Hypercube Inc. Waterloo, Canada 1996.

19 T. Koopmans, *Physica*, 1933, **1**, 104.

Paper 7/01463E; *Received* 3*rd March*, 1997